СООБЩЕНИЯ
ОБЪЕДИНЕННОГО
ИНСТИТУТА
ЯДЕРНЫХ
ИССЛЕДОВАНИЙ
ДУБНА

E2-11275

G.E.Dogotar, R.A.Eramzhyan, H.R.Kissener, R.A.Sakaev

EXCITATION OF THE GIANT RESONANCE IN THE RADIATIVE PION CAPTURE ON 1P SHELL NUCLEI

1978

E2 – 11275

G.E.Dogotar,[1] R.A.Eramzhyan, H.R.Kissener,[2] R.A.Sakaev

EXCITATION OF THE GIANT RESONANCE IN THE RADIATIVE PION CAPTURE ON 1P SHELL NUCLEI

[1] Permanent address: Institute of Applied Physics, Academy of Science, Moldavian SSR, Kishinev

[2] Permanent address: Zentralinstitut für Kernforschung, Rossendorf, DDR.

Доготарь Г.Е. и др. E2-11275

Возбуждение гигантского резонанса в процессе радиационного захвата пионов ядрами 1p -оболочки

Спин-изоспиновые переходы в процессе (π^-,γ) на ядрах мишени ^{6}Li, ^{7}Li, ^{9}Be, ^{11}B, ^{13}C и ^{14}N рассчитаны в рамках модели оболочек. Доминируют переходы, связанные с возбуждением состояний гигантского резонанса. Полученные результаты сравниваются с имеющимися экспериментальными данными. Обсуждаются вопросы гросс-структуры и квантовые числа резонансов, интенсивности переходов и полный выход γ -квантов.

Работа выполнена в Лаборатории теоретической физики ОИЯИ.

Сообщение Объединенного института ядерных исследований. Дубна 1978

Dogotar G.E. et al. E2-11275

Excitation of the Giant Resonance in the Radiative Pion Capture on 1p Shell Nuclei

The spin-dipole transitions in the (π^-,γ) reaction on ^{6}Li, ^{7}Li, ^{9}Be, ^{11}B, ^{13}C and ^{14}N are calculated in the shell model and are compared with experiment. The discussion includes the gross structure and the quantum numbers of the resonance, relative branchings, prominent partial transitions and total yields.

The investigation has been performed at the Laboratory of Theoretical Physics, JINR.

Communication of the Joint Institute for Nuclear Research. Dubna 1978

1. INTRODUCTION

Among the numerous processes occuring in the interaction of particles of intermediate energy with atomic nuclei, one can select a whole family such as photo reactions up to incident energies $E_\gamma \sim 25...30$ *MeV*, electro-excitation at low momentum transfer, muon capture, photo- and electroproduction of pions, radiative pion capture, etc. A common feature of these reactions is the formation of particle-hole states with not very high excitation energy which are produced due to the influence of the external field. The interaction between the particle and the hole under these conditions results in the formation of coherent nuclear states which show up as giant resonances. The structure of the external field acting on the nucleus appears in the specific type (or several types) of collective nuclear motion characterized by angular momentum J, parity π and isospin T.

The appearance of the giant resonance in the photo- and electrodisintegration of nuclei is a well known example. Recently a convincing experimental evidence for the excitation of the giant resonance in muon capture has been obtained. The aim of the present work is to show that the concept of resonance excitation also allows one to describe the basic features of the radiative pion capture process. This paper deals mainly with the spin-dipole resonances connected with the operators $[\sigma \times Y_1]_{K=0,1,2}$. The basic ideas of the conventional theory of radiative pion capture are briefly reviewed in Sec. 2. We consider only 1p shell nuclei using the

shell model approach sketched in Sec. 3. This model was earlier applied to photonuclear reactions where it provided a good description of a large body of data (refs. [1-5]). In Sec. 4 we discuss the spin-dipole resonances in a more general context, referring also to analogous results on photo- and electro-excitation into the giant resonance region. M1 type resonances in the (π^-, γ) process have been considered in a preceding work [6].

2. *BASIC IDEAS OF THE THEORY OF RADIATIVE PION CAPTURE*

The radiative pion capture by atomic nuclei is considered in the impulse approximation. The amplitude of the elementary process on a proton is taken from ref. [7]. The pion wave function is obtained by solving the Klein-Gordon equation with the Kisslinger-Ericson nonlocal optical pion-nucleus potential (see ref. [8]) for details. Mesoatomic parameters, used for calculation of the yield of γ-quanta R) is given in *Table 1*.

Table 1

Mesoatomic parameters $\Lambda_{n\ell}$ and ω_ℓ used in the present calculations

target nucleus	$\hbar\Lambda_{1s}$ [keV]	$\hbar\Lambda_{2p}$ [eV]	ω_s	ω_p
^{6,7}Li	0.195	0.015	0.4	0.6
^{9}Be	0.591	0.16	0.3	0.7
^{11}B	1.680	0.32	0.2	0.8
^{13}C	3.140	1.02	0.15	0.85
^{14}N	4.480	2.1	0.1	0.9

3. *NUCLEAR MODEL*

The nuclear wave functions were represented by nonspurious bound state shell model states obtained by diagonalizing effective Hamiltonians in the full spaces of $0\hbar\omega$ and $1\hbar\omega$ excitations with respect to a ^{4}He core. For A=6, ground state parity wave functions were taken from Barker [9], and the opposite-parity states correspond to a Rosenfeld interaction (ref. [10]). For the nuclei A=7 through 14 we adopted a fixed set of s.p. energies and interaction matrix elements, including the Cohen-Kurath version (8-16)2BME [11] for the interaction within the 1p shell, and a central force of the Gillet type between nonequivalent nucleons. The corresponding strength parameters and s.p. energies are listed in table 1 of ref. [12]. They are close to those used in our previous calculations of photo reactions and muon capture for A= 7, 8, 13 and 14 nuclei (see refs. [1-5]).

4. *RESULTS AND DISCUSSION*

The calculated yield of hard γ quanta in the (π^-,γ) process is presented for the target nuclei ^{6,7}Li, ^{9}Be, ^{11}B, ^{13}C and ^{14}N, together with available data [13,14]. For easier comparison with experimental histograms, theoretical branches to individual final states (vertical bars in the figures) were spreaded with an arbitrary width of $\Delta E = 2$ *MeV* which takes qualitatively into account experimental finite resolution and the decay width since most of the final levels are above the threshold for nucleon emission (note: histograms and smooth curves are in arbitrary units).

Then we discuss the gross structure of the yield R, using the LS coupling scheme which provides a natural description of the observed patterns in terms of the configurational splitting of components with different spatial symmetry [λ]. The LS scheme is further utilized for illustrating the systematics of dominant partial transitions. For the cases A=7 through 14, the structure of

the corresponding states involved is given in *Table 3.* for A=6 it can be seen from ref. [10].

4.1. Gross Structure of the Resonance

For the lightest 1p shell nuclei one expects that the dipole type hole excitations 1s → 1p give the main part of the integral radiative capture rate. With increasing occupation of the 1p valence shell the role of valence excitations 1p→(2s,1d) should become more and more important, whereas the 1s→1p excitations should be gradually blocked. This feature is clearly seen from the structure of final states in the strong partial transitions (*Table 3*). As a consequence, the excitation energy E_x of the main peak should decrease with increasing A which is indeed observed. At the upper end of the 1p shell one expects dipole type valence excitation and

Table 2

Predicted strong partial transitions in the radiative pion capture on ^{6}Li to negative parity levels

J_f	$E_x(^6He)$ [MeV]	R_s	R_p	$R\,[10^{-4}]$	$\frac{R}{R_{tot}(J_f)}$ %	$\frac{R}{R_{tot}}$ %
0⁻	13.9	8.0	1.9	10	50	3
1⁻	13.8	10.7	6.8	18	19	5
	16.0	21	14	35	39	11
2⁻	11.0	24	14	37	36	12
	21.0	10	4.0	14	14	4
	21.6	14	6.6	20	20	6
	29.9	8.9	6.8	16	15	5
3⁻	21.0	15	17	32	81	10

quadrupole type excitation through two oscillator shells to be of comparable weight (see ref. [15]); the latter will be spreaded over a much wider energy range than the dipole transitions and presumably contribute to the long tail in the histograms at lower photon energy.

^{6}Li. The spectrum of hard γ quanta from the ^{6}Li(π^-,γ) reaction shows two well separated regions (*fig. 1a),* apart from the well known M1 resonances (see ref. [6]). The lower part of the intrinsic excitation spectrum (the high-energy end of the primary γ spectrum) is mainly connected with promotion of a 1p nucleon to the (2s,1d) shell $|pd:{}^{33}L_J\rangle$ and also from specific excitation of the $(1s)^4$ core where the states of the intermediate nucleus ^{6}He have maximal spatial symmetry

$$|s^{-1},(p^3[3]\,{}^{22}L_J)\rangle;\qquad p^3[3]\ \text{contains}\ L=1,3\,.$$

Here we used the conventional notation $[\lambda]^{2T+1,2S+1}L_J$.

The second excitation region at higher energy $E_x(^6He)$ is connected with formation of states with lower spatial symmetry

$$|s^{-1}\,,(p^3\,[21]\,{}^{22}L_J)\rangle;\quad p^3[21]\ \text{contains}\ L=1,2\,.$$

Such a structure of the giant resonance is also predicted for photonuclear reactions and for muon capture [10].

Apart from the M1 resonance, the theoretical spectrum at low E_x looks too empty, possibly due to an upward shift of the dominating peak 2^-. Several strong branches to 2^- and 1^- final states but only one to a 3^- level are predicted (*table 2*; see also sec. 4.3.).

A similar upward shift of a strongly excited 2^- level seems to happen in the analogous photo reaction on ^{6}Li. The available photonuclear data on ^{6}Li (quoted in ref. [10]) are however somewhat contradictory and too incomplete to be conclusive concerning the model. The photoneutron cross section obtained with monoenergetic photons (Berman et al., 1975) shows a broad bump around $E_x(^6Li) \approx 12$ *MeV* and ends at 32 *MeV*, below the region of predicted 1s hole excitation. Moreover, the photo-

Table 3

Predicted strong partial transitions in the radiative pion capture on nuclei A=7...14

target	J_f	E_x [MeV] final	R_s	R_p	R $[10^{-4}]$	$\frac{R}{R_{tot}(J_f)}$ %	$\frac{R}{R_{tot}}$ %	structure of final state % $d_{5/2}$	2s	$d_{3/2}$	$(1s)^{-1}$
^{7}Li	$1/2^+$	0.9	7.2	4.9	I2	37	6	I0	79		8
	$3/2^+$	7.I	9.2	5.2	I4	24	7	24	6	68	
		I3.0	6.6	8.0	I5	24	7	49		8	4I
	$5/2^+$	2.9	20	I7	36	4I	I8	75	2I		-
		I7.5	I4	I6	30	34	I4		-		98
	$7/2^+$	I8.8	5.I	6.9	I2	79	6		-		94
^{9}Be	$1/2^+$	I3.7	2.5	3.I	6	26	4	38	5	7	50
	$3/2^+$	5.7	2.3	I.6	4	I4	3	79	I3	8	-
	$5/2^+$	5.5	3.0	3.0	6	I3	5	45	45	8	
		7.4	2.7	2.2	5	II	4	36	60		
		7.6	3.5	I.6	5	II	4	49	43	6	
	$7/2^+$	7.0	4.7	4.7	9	43	7	80	I5	5	-
		8.4	3.4	3.4	7	3I	5	67	3I		-
^{11}B	$1/2^+$	5.9	I.2	5.2	6	29	4				
	$3/2^+$	7.2	3.9	I2	I6	4I	9	40	I7	43	-
	$5/2^+$	5.5	I.7	6.6	8	I4	5	22	75		
		7.7	2.7	8	II	I8	6	87	II		-
	$7/2^+$	4.I	I.3	5.5	7	20	4	95			-
		6.5	I.3	5.7	7	20	4	82	8	I0	-
		7.9	I.0	4.4	5	I6	3	83	7	I0	-
		9.3	I.5	7.4	9	25	5	35	7	58	-

Table 3 (continued)

target	J_f	E_x [MeV] final	R_s	R_p	R $[10^{-4}]$	$\frac{R}{R_{tot}(J_f)}$ %	$\frac{R}{R_{tot}}$ %	structure of final state % $d_{5/2}$	2s	$d_{3/2}$	$(1s)^{-1}$
^{13}C	$1/2^+$	II.9	I.5	3.7	5	2I	3	9	42	49	-
	$3/2^+$	3.9	I.0	3.9	5	7	3	67	28	5	-
		5.5	I.9	I0	I2	I8	7	34	64		
		8.0	I.9	8.5	I0	I6	6	56	4I		
		I0.6	I.8	9	II	I7	7	36	I4	50	-
	$5/2^+$	6.4	4	20	24	43	I5	67	29		-
		8.5	I.2	7	8	I4	5	36	52	I2	-
		II.6	I.2	8	9	I6	5	47	4	50	-
^{14}N	2^-	I4.5	I.3	8	9	I5	4	89	5	6	-
		I7.7	I.2	7	8	I3	4	63	32	5	-
		I8.3	I.5	9	I0	I6	5	85	6	9	-
	3^-	6.73	I.4	I0	II	I7	5	95	-	5	-
		I4.9	I.7	II	I2	I9	6	47	22	3I	-
		I5.9	I.4	9	I0	I5	5	4I	7	52	-

neutron data exhaust only a fraction of the total photo strength; from the predicted structure of intermediate states cluster emission and three-body breakup should compete with nucleon emission.

One should note that the theoretical understanding of the giant resonance in the $A=6$ system is still rather qualitative. Both the sequence and structure of low-lying negative parity states in ^{6}Li are very sensitive to details of the residual interaction. Knowledge of the $^{6}Li(ee')$ cross section through the giant resonance region with an accuracy similar to that for ^{12}C and ^{13}C would be of great value, in order to check the model and to compare with the (π^-,γ) data.

The measured 1s -orbital capture distribution (*fig. 1b*) shows the same gross structure as the R_s+R_p distribution in *fig. 1a*, apart from poorer statistics due to coincidence with the pionic $2s \rightarrow 1s$ X -ray. The relative ratio of the strongest partial branches R_{1s} is roughly the same as for the quantities R_s+R_p; only the single 3^- ($\Delta J=2$) peak is more suppressed in s -orbital capture than the peaks 2^- and 1^- which follows from angular momentum consideration.

^{7}Li. The experimental $^{7}Li(\pi^-,\gamma)$ yield (*fig.2*) can also be interpreted in terms of configurational splitting.
a) valence excitations $|(p^2[2]L'),d$ or $2s:L_J>$, $L'=0,2$;
b) hole excitations $|s^{-1},(p^4[31]L'):L_J>$, $L'=1,2,3$.
The symmetry $p^4[4]$ cannot occur because of $T_f=3/2$.

In contrast to the $A=6$ case, the yield in the low-energy region $E_x \approx 0...12$ *MeV* is overestimated, although the M1 g.s. transition ($3/2^-$) is suppressed by orbital symmetry [6]. The main peak is predicted to be a $5/2^+$ level and to correspond mainly to $p_{3/2} \rightarrow d_{5/2}$ transition but turns out to be at too low E_x by at least 4 *MeV*. The peak at $E_x \gtrsim 15$ *MeV* is mainly hole excitation (table 3).

One should note that the specific interaction used for $A=7$ through 14 is not optimal for the $A=7$ case. This already holds for the ^{7}Li g.s. which is not too well represented by Cohen-Kurath wave functions. Utilizing another set of interaction parameters proposed by Ku-

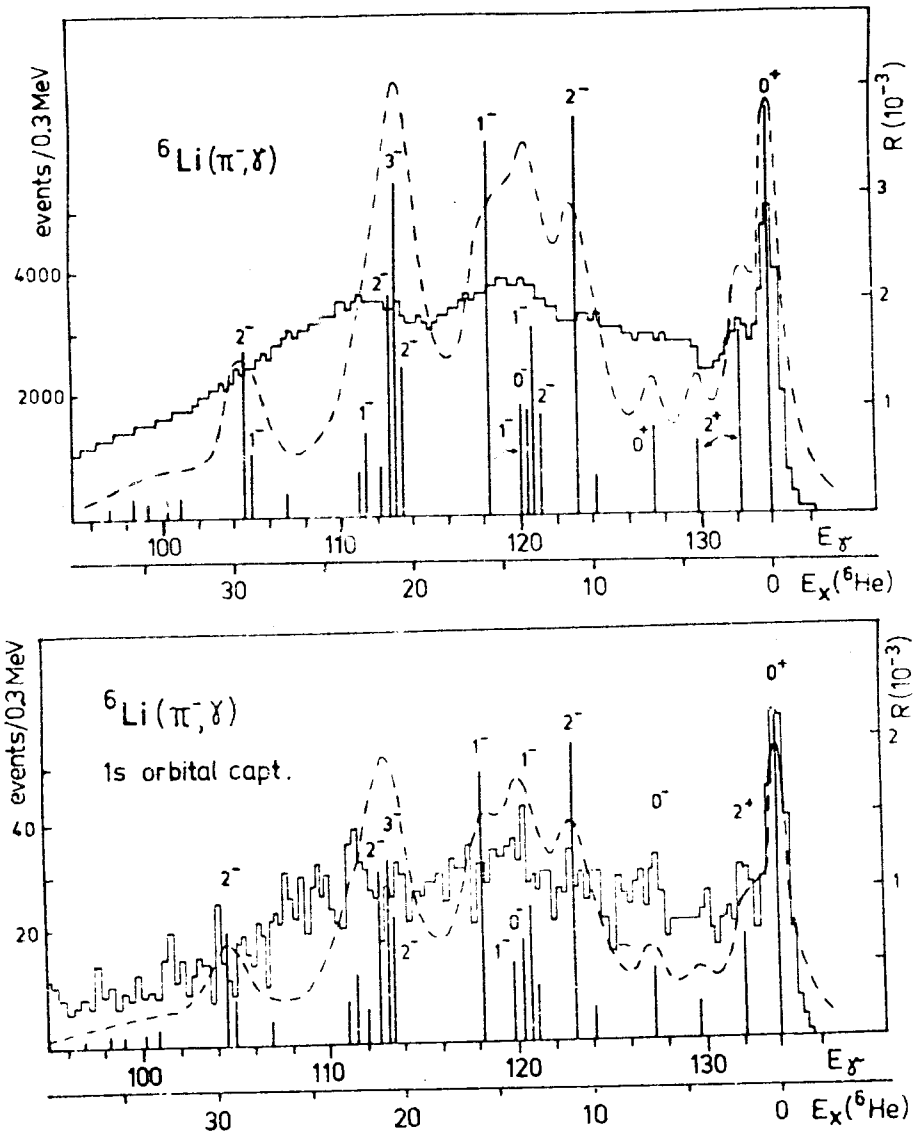

Fig. 1. Radiative pion capture yield on ^{6}Li. The histograms are from SIN, ref. [13]. Theoretical branches (vertical bars) are spreaded over Breit-Wigner shapes (dashed curves); see text. a) total yield R , b) 1s – orbital capture yield $R_{1s}=\lambda_{1s}/\Lambda_{1s}\cdot\omega_{1s}$; $\omega_{1s}=0.335$.

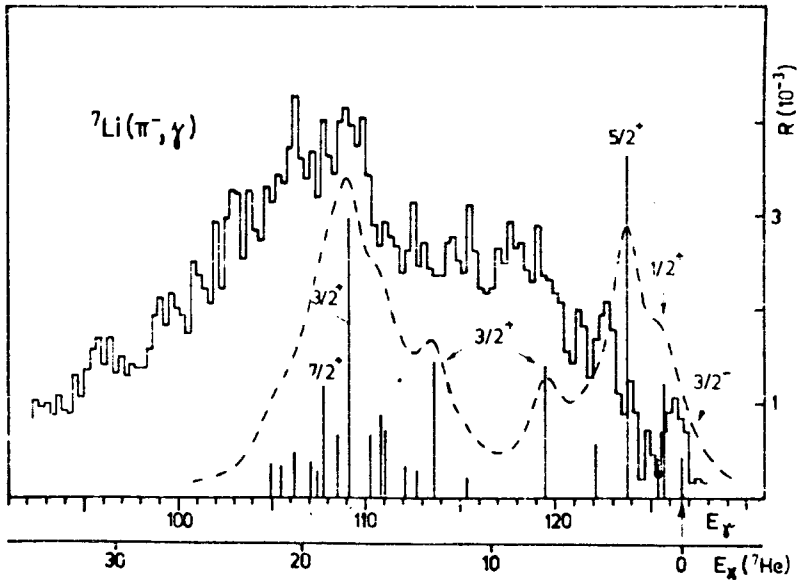

Fig. 2. Radiative pion capture yield on ^{7}Li. *See text to fig. 1.*

rath /16/ provides the required upward shift of the strong $5/2^+$ peak (see refs. /17,18/). Since the calculated (π^-,γ) distribution is also sensitive to the s.p. energies adopted, this point requires further investigation.

The analogous photo excitation in ^{7}Li is not very conclusive concerning the model; our calculated E1 strength distribution to $T_f=3/2$ states is consistent with the photoneutron curve which shows a broad bump around $E_x(^7\text{Li}) \approx 17$ *MeV* but ends below the predicted group of hole excitations. As for ^{6}Li, from the structure of intermediate states the three-body breakup should take an appreciable part of the total photo cross section.

^{9}Be. The theory reproduces the (π^-,γ) data rather well (*fig. 3*), the same holds for photo reactions as will be discussed elsewhere. Compared with the A=6 and 7 cases, the main peak is now at much lower E_x and consists of valence excitation. The configurational splitting

is still clearly present (see table 3). However, only one level ($1/2^+$ at $E_x \approx 14$ *MeV*) with notable $(1s)^{-1}$ structure carries a large (π^-,γ) yield.

^{11}B. For the A=11 case we have bad agreement with the measured (π^-,γ) peak position, using the central interaction (*fig. 4*). One expects some similarity to the A=7 case since the A=11 g.s. contains an additional quartet of nucleons with orbital symmetry /4/. As for A=7, the theoretical yield shows strong valence excitations at too low E_x. The g.s. transition ($1/2^+$) is almost pure $p_{3/2} \to 2s$ but has negligible strength. The next predicted positive parity levels ($5/2^+$ at $E_x \approx$ ≈ 0.4 *MeV* and $7/2^+$ at ≈ 4 *MeV*) are of $p_{3/2} \to d_{5/2}$ type. A quite unusual feature of the predicted dominant transition is the low spin value $J_f = J_i\,(=3/2)$. However, since both wave functions involved contain many compo-

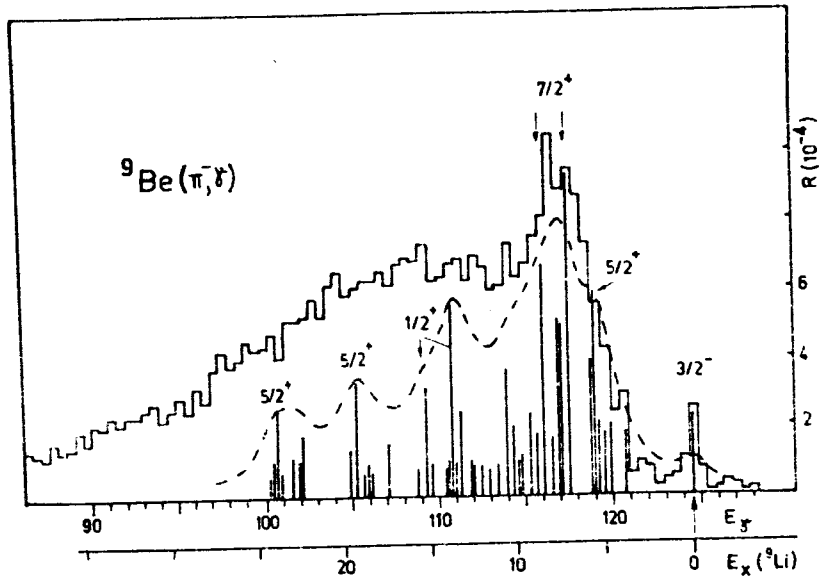

Fig. 3. Radiative pion capture yield on ^{9}Be. *See text to fig. 1.*

nents with comparable weight, a slight change of the interaction parameters might cause major redistribution of the partial strength. For the hole excitations no concentration of (π^-,γ) strength is obtained (see table 3).

The photonuclear data on ^{11}B are also badly reproduced using central interaction. Although the predicted strongest photo absorption lines correspond to $J_f = J_i + 1$ as is usual for dipole transitions the calculated cross section again peaks at much lower $E_x(^{11}B)$ than the measured one.

As was suggested by Kurath[16], the use of non-central components in the residual interaction improves the description of opposite-parity levels (see also ref.[12]) and of the electro-excitation data[19] for the ^{11}B nucleus.

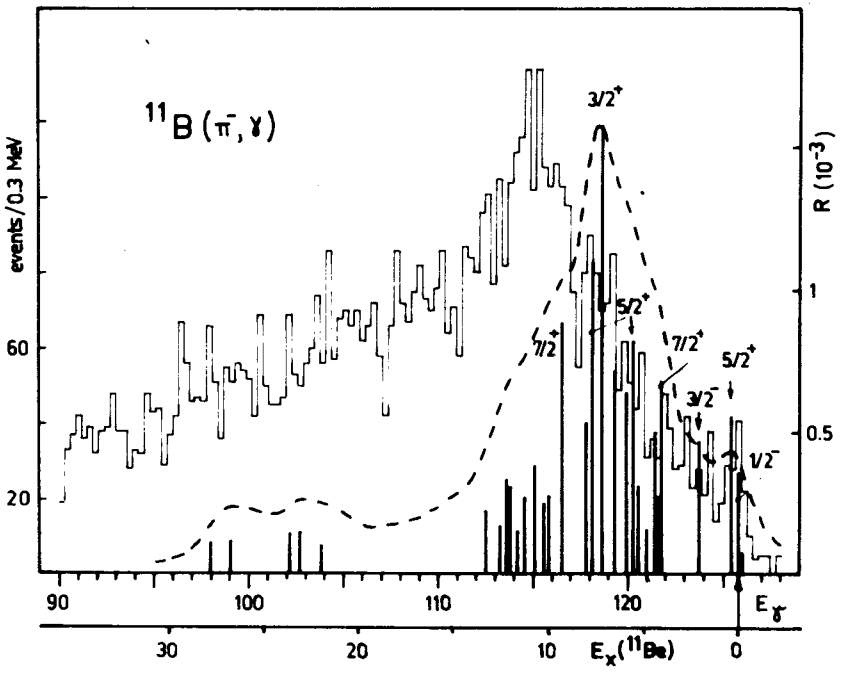

Fig. 4. Radiative pion capture yield on ^{11}B. *See text to fig. 1.*

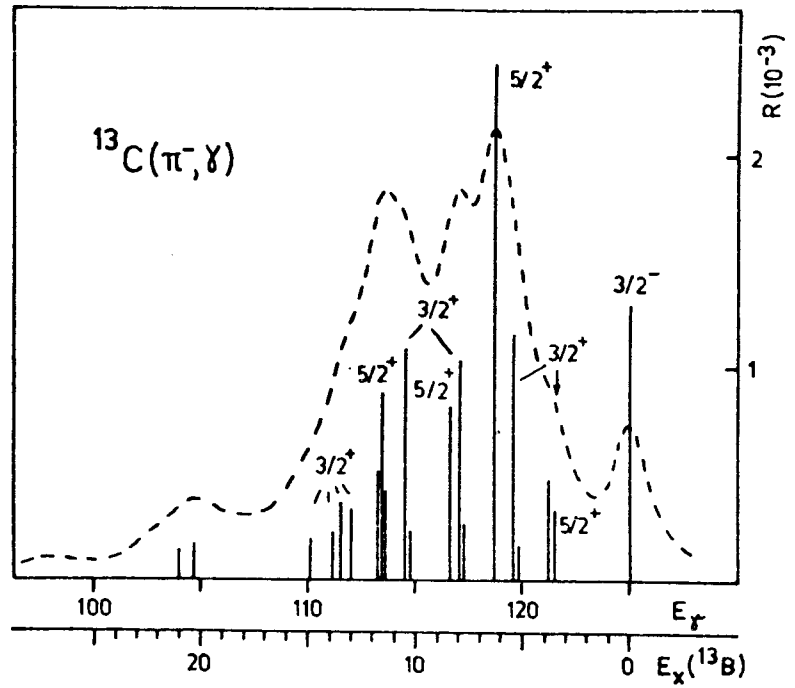

Fig. 5. Calculated radiative pion capture yield on ^{13}C . *See also fig. 1.*

The influence of this new set of interaction parameters on the photo absorption and (π^-,γ) cross sections for ^{11}B will be discussed elsewhere.

^{13}C. For the $A=13$ system one expects similar gross structure of the cross sections as for $A=9$, by adding a quartet of nucleons with symmetry [4]. Our predicted $^{13}C(\pi^-,\gamma)$ yield is shown in *fig. 5*, no data are available at present. As is seen from table 3, the dominating partial transitions have no $(1s)^{-1}$ components.

Because of the detailed data available on ^{13}C for photo reactions and for (ee′) over the giant resonance region, this nucleus is very interesting for comparing all reactions including the (π^-,γ) one. Therefore, a measurement of the $^{13}C(\pi^-,\gamma)$ yield would provide valuable

information. Our calculated photo- and (ee′) cross sections describe the data rather well; details will be given in a forthcoming paper.

^{14}N. *Fig. 6* shows recent SIN data [13], together with our calculation. The position of the maxima and the shape is fairly well reproduced up to $E_x(^{14}C) \approx 20$ *MeV*. No 1s hole excitation is predicted.

In a similar calculation by Baer et al. [20] which is based on the same shell model space but uses a modified Kuo interaction, the Berkeley data are also well reproduced. However, the data were renormalized by subtracting a fitted pole model distribution which is to account for a direct reaction component. As compared with ref. [20] we get a more spreaded strength distribution, without making pole model fits. Also we find more prominently populated 3^- states; the lowest one (E_x=6.73 *MeV*) overlaps with the M1 doublet [6] at 7 and 8 *MeV*. This 3^- level is also seen in the muon capture on ^{14}N [5,21].

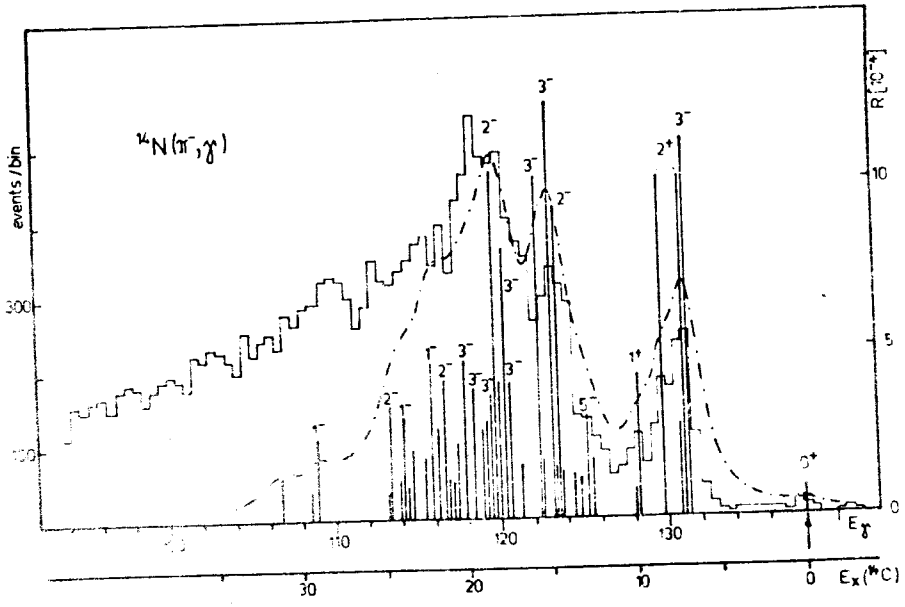

Fig. 6. Radiative pion capture yield on ^{14}N. *See text to fig. 1.*

In the analogous photo reaction on ^{14}N the gross structure of the data is also reproduced [1], although the experimental main peak is about 1 *MeV* above the calculated one.

4.2. *The Low-Energy Tail in the γ Spectra*

The calculated γ yield in the region E_x above the main maximum of the dipole resonance is generally too empty as compared with experiment. The long tail in the histograms is presumably due to $2\hbar\omega$ quadrupole transitions which lie above the intrinsic dipole excitations and are related to the operator $[\sigma \times Y_2]_{K=1,2,3}$, and also to contributions from the direct reaction mechanism. This point was illustrated by a recent calculation for ^{16}O (ref. [15]), using an oscillator space up to $2\hbar\omega$ and Tabakin interaction. According to ref. [15], the $2\hbar\omega$ transitions contribute about 40% of the dipole transition strength and are spreaded over a wide energy range.

4.3. *Quantum Numbers of the Resonances*

In the photonuclear reactions the transitions are of the electric dipole (Y_1) type, and the main contribution in the region of the giant resonance is connected with excitation of states with $J_f = J_i + 1$. In the radiative pion capture process the external field is the axial vector, and the transition operator involves the nucleon spin. In the 1p shell nuclei the main contribution in the giant resonance region is due to the operator

$$[\sigma \times Y_1(\hat{r})]_{0^-,1^-,2^-}$$

which can lead to states with $J_f = J_i + 2$. Due to the statistical factor these transitions should be rather strong. However, as can be seen from figures 1 through 6, this feature is not realized in all cases, and this is related

to the structure of the target ground state. In order to illustrate the situation we employ the LS coupling scheme for the description of the nuclear states. As is known, in the g.s. of 1p shell nuclei there are usually one of two leading components [22]:

$$^{6}\mathrm{Li}:\ \Psi(1^{+}0) \sim 0.97\,|p^{2}[2]\,^{13}S_{1}>;$$

$$^{7}\mathrm{Li}:\ \Psi(3/2^{-}1/2) \sim 0.99\,|p^{3}[3]\,^{22}P_{3/2}>;$$

$$^{9}\mathrm{Be}:\ \Psi(3/2^{-}1/2) \sim 0.90\,|p^{5}[41]\,^{22}P_{3/2}> -0.40\,|[41]\,^{22}D_{3/2}>;$$

$$^{11}\mathrm{B}:\ \Psi(3/2^{-}1/2) \sim 0.64\,|p^{7}[43]\,^{22}P_{3/2}> + 0.57\,|[43]\,^{22}D_{3/2}>;$$

$$^{13}\mathrm{C}:\ \Psi(1/2^{-}1/2) \sim 0.80\,|p^{9}[441]\,^{22}P_{1/2}> -0.43\,|[432]\,^{24}D_{1/2}>;$$

$$^{14}\mathrm{N}:\ \Psi(1^{+}0) \sim 0.95\,|p^{10}[442]\,^{13}D_{1}> - 0.25\,|[433]\,^{11}P_{1}> -$$

$$-0.20\,|[442]\,^{13}S_{1}>; \qquad (4)$$

Since the final states have isospin $T_f = T_i + 1$ in the cases considered, the number of configurations reached by the operator $[\sigma \times Y_1]$ is rather limited.

A=6: The excitation of valence nucleons predominantly leads to configurations $|s^{4}pd:\,^{33}L_{J}>$ and $|s^{4}pd:\,^{31}L_{J=L}>$ where the orbital momentum must be equal to $L=1$, due to the selection rule $\Delta L=1$ for the operator $[\sigma \times Y_1]_K$, together with the vanishing orbital momentum in the ^{6}Li g.s. (see eq. (4)). The main spin-dipole strength in the low-energy region of the intermediate nucleus ^{6}He should therefore be connected with states 2^{-} and 1^{-}, i.e., $\Delta J \leq 1$. For the other low-lying configuration

$$|s^{-1}, p^{3}[3]\,^{22}P_{J'=1/2,3/2} : P_{J=0,1,2}>$$

we also have $\Delta J \leq 1$.

The second excitation region which corresponds to 1s hole excitation with lower orbital symmetry is mainly described by the configurations

$$|s^{-1}, p^{3}[21]\,^{22}P:\,^{33}P_{J}> \text{ and } |s^{-1}, p^{3}[21]\,^{22}P:\,^{31}P_{J=1}>.$$

Again, the total final spin cannot exceed the value $J_f = 2^{-}$. Only one state with the configuration

$$|s^{-1}, p^{3}[21]^{24}P:\,^{35}P_{J}>$$

corresponds to the quantum numbers 3^{-}, i.e., $\Delta J = 2$. Therefore, in the $^{6}\mathrm{Li}(\pi^{-}, \gamma)$ process the giant resonance is mainly connected with states $J_f = 2^{-}$ as for photo absorption, and only one partial transition can feed a 3^{-} level.

A=7: An analogous situation occurs in the ^{7}Li case. The valence nucleon excitation mainly feeds the configurations

$$|s^{4}, (p^{2}[2]^{31}S), d:\,^{42}D_{3/2,5/2}> \text{ and } |s^{4}, (p^{2}[2]^{31}D), d:\,^{42}L_{J}>.$$

In the latter case, due to the structure of the g.s. and the $\Delta L=1$ rule, L can take the values 0, 1 and 2, and the total spin J_f cannot exceed the value $5/2^{+}$. Therefore, the low-energy region of ^{7}He should not have resonances with $\Delta J=2$.

The hole excitations can lead to the configurations

a) $|s^{-1}, p^{4}[31]^{33}L:\,^{42}L>$,

b) $|s^{-1}, p^{4}[31]^{33}L:\,^{44}L>$,

c) $|s^{-1}, p^{4}[31]\,^{31}L':\,^{42}L'>$,

the symmetry $p^{4}[4]$ cannot occur because of $T_f = 3/2$. The Young scheme $p^{4}[31]$ allows orbital momenta 1,2 and 3; because of the g.s. momentum $L_i = 1$ and the selection rule $\Delta L=1$ both L and L′ can take the values 1 and 2. Hence, the configurations a) and c) again give spin J_f only up to $5/2^{+}$, i.e., $\Delta J \leq 1$. In the configuration b) a total spin $7/2^{+}$ occurs for $L=2$, but this state has poorer overlap with the g.s. than the states with lower L. Therefore one expects for the $^{7}\mathrm{Li}(\pi^{-}, \gamma)$ reaction

a weak partial transition $\Delta J=2$ to a configuration $|s^{-1}, p^4[31]^{33}D : {}^{44}D_{7/2}>$ and several stronger resonances with lower total angular momentum.

A=9.: In the ^{9}Be nucleus, as well as in heavier nuclei, the g.s. also contains a notable component $L=2$ which will mainly provide the excitation of resonances with $\Delta J=2$. With increasing weight of this $L=2$ component the strength of the $\Delta J=2$ resonances should also increase. For ^{9}Be one of the $\Delta J=2$ resonances is connected with the leading P component in the g.s. and corresponds to the transition $^{22}P_{3/2} \rightarrow {}^{44}D_{7/2}$.

A=11: Since the g.s. contains two components $L=1$ and 2 of the comparable amplitude, no systematics of partial transitions can be predicted. The total strength will be spreaded over many groups of levels with different spins, and the distribution will sensitively depend on detailed final state structures.

A=13: The $^{13}C(\pi^-, \gamma)$ case should be particularly mentioned. Because of the g.s. spin $1/2^-$ the $\Delta J=2$ resonance is already connected with the leading $^{22}P_{1/2}$ component in the g.s. wave function

$$|p^9[441]^{22}P_{1/2}> \rightarrow |p^8[431], d : {}^{42}D_{5/2}>;$$

it should dominate in the excitation spectrum.

The hole excitations

$$|s^{-1}, (p^{10}[442]^{31}L) : {}^{42}L_J>, \quad L=0,2$$

have minor weight but can also lead to $\Delta J=2$ final states via the configurations with $L=2$.

A=14: From the leading component $|p^{10}[442]^{13}D_1>$ of the ^{14}N g.s. one can reach final levels $J=0^- \ldots 3^-$ through the operator $[\sigma \times Y_1]$, with configurations

$$|(p^9[441]L'), d : {}^{31}L_J \text{ or } {}^{33}L_J>, \quad L'=1,3$$

and

$$|(p^9[432]L'), d : {}^{31}L_J \text{ or } {}^{33}L_J>, \quad L'=1,2.$$

The hole excitations can only contribute to resonances with $\Delta J \leq 1$

$$|s^{-1}, p^{11}[443]^{22}P : {}^{33}P_{J=0,1,2}>.$$

4.4. *Total Capture Rates and Distribution Over Final Spins*

The calculated total (π^-, γ) yields for the nuclei considered (see *Table 4*) agree with the available experimental values [14], without making pole model subtractions. Estimates of the contribution of direct excitation mechanism give an order of magnitude less than that of the resonance mechanism [23]. The inclusion of $2\hbar\omega$ final states for the $^{16}O(\pi^-, \gamma)$ reaction gives an increase of the total yield by about 40% (ref. [15]). Assuming the same relative amount from quadrupole transitions also for the other cases, one even would overestimate the measured total yields. For photo absorption and muon capture yields one usually finds similar overestimates.

Table 5 shows the strength distribution to groups of levels with the same spin J_f; column 7 of table 3 illustrates the relative concentration of the strength to individual levels within each group J_f. The qualitative behaviour was already discussed in the preceding section. Except for A=14, the relative distribution of both R_s and R_p over the J_f values peaks at $J_f = J_i + 1$. For A=14 this still holds for R_s, but the dominating part R_p peaks at $J_f = J_i + 2$ due to the leading D component in the ^{14}N g.s. Another anomaly for A=13 is due to the g.s. spin value 1/2; here the sum to $J_f = J_i + 2$ is about the same as the $J_i + 1$ sum, and even levels with $J_f = J_i + 4$ are populated, as in the A=14 case.

Table 4

Total radiative pion capture rates calculated for all $0\hbar\omega$ and $1\hbar\omega$ final states. Comparison with experimental data

target J_i	number of final levels ($T_f = T_i + 1$)		R_s [10^{-3}]			R_p [10^{-3}]			R_{total} [10^{-3}]	
	$0\hbar\omega$	$1\hbar\omega$	$0\hbar\omega$	$1\hbar\omega$	sum	$0\hbar\omega$	$1\hbar\omega$	sum	calc.	exp.
^{6}Li 1^+	5	47	4.3	15.2	19.5	3.0	9.9	12.9	32.4	34 ± 2 a)
^{7}Li $3/2^-$	5	74	0.47	10.4	10.9	0.61	9.4	10.0	20.9	19 ± 2 a)
^{9}Be $3/2^-$	19	294	0.51	6.3	6.8	0.39	5.7	6.1	12.9	
^{11}B $3/2^-$	19	455	0.49	3.2	3.7	1.1	12.4	13.5	17.2	
^{13}C $1/2^-$	5	241	0.39	2.6	3.0	0.95	12.7	13.6	16.6	
^{14}N 1^+	5	191	0.59	2.8	3.4	2.1	15.4	17.5	20.9	21.3 ± 2.1 a)

a) ref. [14]

Table 5

Calculated (π^-, γ) yield distribution to groups of opposite-parity levels J_f, $T_f = T_i + 1$

target J_i	J_f	nr of levels	R_s	R_p [10^{-3}]	$R(J_f)$	target J_i	J_f	nr of levels	R_s	R_p [10^{-3}]	$R(J_f)$
^{6}Li 1^+	0^-	7	1.4	0.4	1.8	^{11}B $3/2^-$	$1/2^+$	77	0.5	1.7	2.2
	1^-	14	5.6	3.4	9.0		$3/2^+$	119	0.8	3.1	3.9
	2^-	15	6.4	3.9	10.3		$5/2^+$	117	1.3	4.6	5.9
	3^-	8	1.8	2.1	3.9		$7/2^+$	82	0.6	2.9	3.5
	4^-	3	0.0	0.1	0.2		$9/2^+$	44	0.0	0.2	0.2
	Σ	47	15.2	9.9	25.1		$11/2^+$	16	-	-	-
							Σ	455	3.2	12.4	15.7
^{7}Li $3/2^-$	$1/2^+$	17	1.9	1.4	3.3	^{13}C $1/2^-$	$1/2^+$	44	0.4	2.0	2.5
	$3/2^+$	24	3.3	2.8	6.1		$3/2^+$	67	1.3	5.3	6.6
	$5/2^+$	20	4.6	4.3	8.9		$5/2^+$	64	0.8	4.8	5.7
	$7/2^+$	10	0.6	0.9	1.5		$7/2^+$	44	0.0	0.3	0.3
	$9/2^+$	3	0.	0.	0.1		$9/2^+$	22	0.0	0.2	0.2
	Σ	74	10.4	9.4	19.8		Σ	241	2.6	12.7	15.3
^{9}Be $3/2^-$	$1/2^+$	54	1.2	1.0	2.2	^{14}N 1^+	0^-	19	0.2	0.5	0.6
	$3/2^+$	82	1.5	1.4	2.8		1^-	45	0.7	3.0	3.7
	$5/2^+$	77	2.6	2.1	4.7		2^-	53	1.2	5.2	6.4
	$7/2^+$	50	1.1	1.1	2.2		3^-	41	0.8	5.9	6.7
	$9/2^+$	24	0.0	0.1	0.1		4^-	24	0.0	0.5	0.5
	$11/2^+$	7	-	-	-		5^-	9	-	0.3	0.3
	Σ	294	6.3	5.7	12.0		Σ	191	2.8	15.4	18.2

5. SUMMARY

The calculation of radiative pion capture on 1p shell nuclei presented in this paper is based upon the concept of resonance mechanism. The theory describes the gross structure of the nuclear excitation spectra; the agreement with dealed data demonstrates that the excitation of the giant resonance plays an important role in this process. Our general finding is that the calculated (π^-, γ) yield distributions describe the data well in those cases where also the photonuclear data are well reproduced, although the amplitudes of the elementary processes are different.

In the cases considered, the best agreement is obtained for $A = 9$ and 14. The configurational splitting of the resonances is clearly seen in the $A = 6$ and 7 cases, to somewhat less extent also for $A = 9$. For heavier nuclei the contribution from hole excitation is small and is spreaded out. For $A = 7$ and 11 the calculated main peaks are at too low intrinsic excitation energies as compared with histograms.

In all cases the calculated spectra at energies E_x above the main maximum are too empty, presumably due to the neglect of quadrupole transitions.

The systematics of spins predicted for the resonances is well understood in terms of the structure of the target g.s. and of the selection rule for the leading term of the transition operator. For $A = 9$, 13 and 14 the strongest predicted partial transitions are to levels $J_f = J_i + 2$, and for $A = 6,7$ to levels $J_f = J_i + 1$. The exceptional case $A = 11$ needs further investigation. The predicted strong partial transitions suggest experimental checking of spin predictions through selected coincidence experiments. This point will be discussed in a forthcoming paper.

REFERENCES

1. *Jager H.U., Kissener H.R., Eramzhyan R.A. Nucl. Phys., 1971, A171, p.584.*
2. *Eramzhyan R.A., Jager H.U., Kissener H.R. Proc. Int. Seminar "Electromagnetic Interactions of Nuclei at Low and Intermediate Energies", Moscow, 1971, p.63; JINR, P4-6941, Dubna, 1972.*
3. *Aswad A. et al. Nucl.Phys., 1973, A208, p.61.*
4. *Kissener H.R. et al. Nucl.Phys., 1974, A219, p.601.*
5. *Kissener H.R. et al. Nucl.Phys., 1973, A215, p.424.*
6. *Dogotar G.E. et al. JINR, E2-10509, Dubna, 1977, submitted to Nucl.Phys.*
7. *Maguire W., Werntz C. Nucl.Phys., 1973, A205, p.211.*
8. *Dogotar G.E. et al. Nucl.Phys., 1977, A282, p.474.*
9. *Barker F.C. Nucl.Phys., 1968, 83, p.418.*
10. *Sakaev R.A., Eramzhyan R.A. JINR, P2-9610, Dubna, 1976.*
11. *Cohen S., Kurath D. Nucl.Phys., 1965, 73, p.1.*
12. *Jager H.U., Kirchbach M. ZfK-321 (1977). Nucl. Phys. (in print).*
13. *Alder J.C. et al. Proc. VII Int. Conf. on High Energy Physics and Nuclear Structure, Contr. C-14, Abstracts p.43, Zurich, 1977.*
    Alder J.C. et al. Proc. Int. Top. Conf. on Meson-Nuclear Physics,, Pittsburgh (1976), p.626.
14. *Baer H.W. et al. Phys. Rev., 1973, C8, p.2029.*
    Baer H.W., Growe K.M., Truol P. Adv. in Nuclear Physics, ed. M.Baranger and E.Vogt, Plenum Press, 1977, vol.9, p.171.
15. *Eramzhyan R.A. et al. Nucl.Phys., 1977, A290, p.294.*
16. *Millener D.J., Kurath D. Nucl.Phys., 1975, A255, p.315.*
17. *Kirchbach M., Kissener H.R. ZfK-336 (1977), p.111.*
18. *Dogotar G.E. et al. ZfK-336 (1977), p.113.*
19. *Teeters W.D., Kurath D. Nucl.Phys., 1977, A283, p.1.*
20. *Baer H.W. et al. Phys. Rev., 1975, C12, p.921.*
21. *Bellottii E. et al. SIN Physics Report No. 1 (Dec. 1976), p.41.*
22. *Bojarkina A.N. Izv. Akad. Nauk SSSR, ser. fiz., 1964, 28, p.337.*
23. *Wunsch R. Nucl.Phys., in print.*

Received by Publishing Department on January 19, 1978.